Investigating Mach-Zehnder Interferometers in Silicon-on-Insulator Photonics Platform

Eliezer Shahid, *Spark Photonics Design Inc.*

***Abstract*— The following report will propose a design of experiment to study the performance of Mach-Zehnder Interferometers by varying the length of one of the arms to extreme values and collecting the results from simulation and then verifying those results with experimental ones. The purpose of this is to extract material data from experimental data. Parameters that will be varied will be waveguide length for the delay arm.**

I. INTRODUCTION

Interferometers are a fundamental component within the realm of integrated photonics. These devices, and the many configurations they come in, are key to making components such as optical modulators, switches, and sensors. The study of the Mach-Zehnder Interferometer will teach us how it operates and will help us to learn how changing different parameters will yield different outcomes.

II. MACH-ZEHNDER INTERFEROMETER

A Mach-Zehnder Interferometer (MZI), in the simplest terms, splits light into two, sends it down two waveguides, and then recombines them at the end. An ideal device, when balanced, will give us the same output for the given input. Figure 1 shows what a balanced MZI looks like.

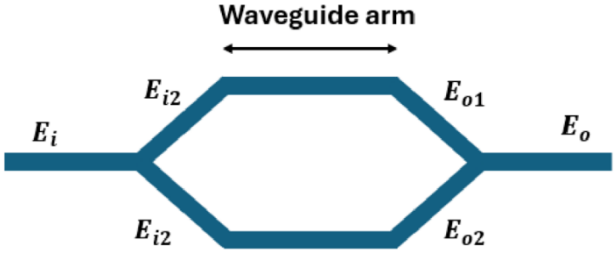

Fig. 1. MZI in a balanced configuration [2]

A balanced MZI just means that both waveguides that come between the two splitters are the same length and have the same properties. The signals that run through the two waveguide arms will constructively combine in the MZI output. The output will be the same as the input in an ideal scenario.

The opposite of a balanced MZI is an unbalanced MZI. This just means that one of the arms has a different length than the other, and this can cause the signal to interfere with each other in a variety of different ways, based on the difference between the lengths of the arms. Figure 2 illustrates an unbalanced MZI.

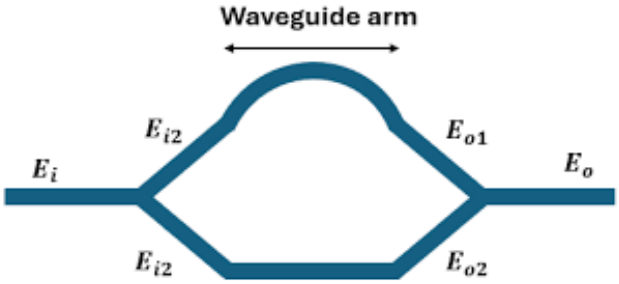

Fig. 2. MZI in an unbalanced configuration [2]

To understand the MZI, we must first look at the splitter for our device. The y-splitter, a splitter we will be using in our device has an input intensity I_i and an electric field E_i. When the light is split into the two branches, it is split equally. The intensity and electric field in each waveguide arm can be described as:

$$I_1 = I_2 = \frac{I_i}{2}$$

$$E_1 = E_2 = \frac{E_i}{\sqrt{2}}$$

When light is combined with a y-splitter at the end of our device, the electric field can be described as:

$$E_{o1} = \frac{E_1}{\sqrt{2}} \quad \& \quad E_{o2} = \frac{E_2}{\sqrt{2}}$$

$$E_o = \frac{E_1 + E_2}{\sqrt{2}}$$

This can then be changed into the following form which describes its behavior in terms of the propagation constant

$$\beta = \frac{2\pi n}{\lambda}.$$

$$E_{o1} = E_1 e^{-i\beta L_1} = \frac{E_i}{\sqrt{2}} e^{-i\beta L_1}$$

$$E_{o2} = 2e^{-i\beta L_2} = \frac{E_i}{\sqrt{2}} e^{-i\beta L_2}$$

$$E_o = \frac{E_1 + E_2}{\sqrt{2}} = \frac{E_i}{2}(e^{-i\beta L_1} + e^{-i\beta L_2})$$

The intensity can be described as the following:

$$I_o = \frac{I_i}{4}|e^{-i\beta L_1} + e^{-i\beta L_2}|^2$$

$$I_o = \frac{I_i}{2}[\,1 + \cos(\beta \Delta L)]$$

The expression above is in the case where $\Delta L = L_2 - L_1$ and $\beta = \beta_1 = \beta_2$.

III. Modeling & Simulation

The first step in our study is to model a waveguide and simulate it to understand its performance. The waveguide we have modeled is based on the waveguide that will be available to us during the fabrication process. The waveguide is 500nm wide and 220nm tall rectangular waveguide made of Silicon; the cladding is made of Silicon Dioxide. The width of 500nm is chosen because it does a great job of confining a single TE mode inside of the waveguide. Figure 3 shows the mode profile of the waveguide from Lumerical MODE simulations.

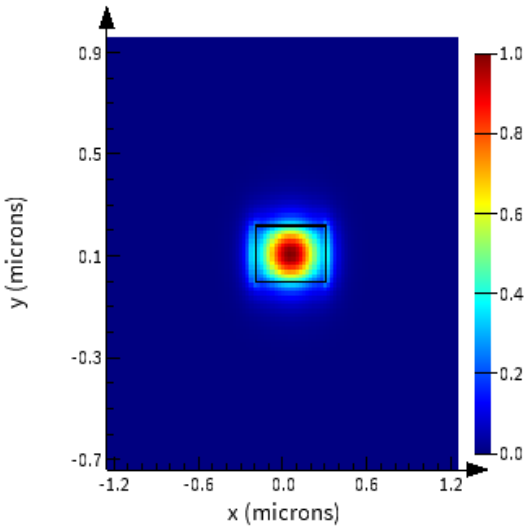

Fig. 3. Waveguide mode profile for a quasi-TE mode

The mode simulation was run with the center wavelength set to 1550 nm, then a wavelength sweep was conducted between 1500nm and 1600nm to account for material and waveguide dispersions. Figure 4 and Figure 5 show the effective index and group index of the waveguide.

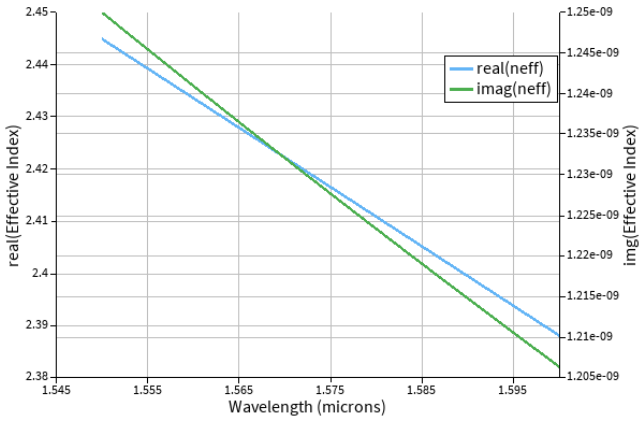

Fig. 4. Effective index vs. wavelength for a TE mode

This chart shows the effective index of our waveguide swept over a range of wavelengths. We can see the real and imaginary index for our waveguide, both of which are decreasing over the wavelengths.

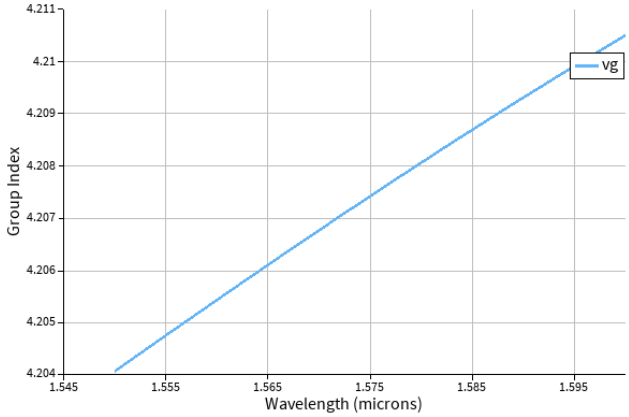

Fig. 5. Group index vs. wavelength for a TE mode

We use MATLAB to then determine the compact model of our waveguide. The model is expressed as a 2nd order polynomial that comes from a Taylor expansion around the center wavelength, which in our case is 1550 nm.

$$n_{eff}(\lambda) = n_1 + n_2\,(\lambda - \lambda_0) + n_3\,(\lambda - \lambda_0)^2$$

$$n_{eff}(\lambda) = 2.44 + 1.33\,(\lambda - 1550) - 0.04\,(\lambda - 1550)^2$$

The transfer function for the MZI comes from the expression we derived earlier in this paper describing the intensity of an MZI. The equation is shown below.

$$I_o = \frac{I_i}{2}[\,1 + \cos(\beta \Delta L)]$$

When you divide both sides of this expression by I_i, we get the transfer function, where $\frac{I_o}{I_i}$ describes the ratio between the output and input intensity.

$$\frac{I_o}{I_i} = \frac{1}{2}[\,1 + \cos(\beta \Delta L)]$$

The Free Spectral Range or FSR is described as:

$$FSR = \frac{\lambda^2}{n_g \Delta L}$$

After completing waveguide simulations, we then simulate a few circuits in Luceda IPKISS [7], a photonic layout software that has circuit simulation capabilities. Figure 6 shows the layout for an MZI in IPKISS with a 1000um long arm. Figure 7 shows the code that calls the simulation for the device.

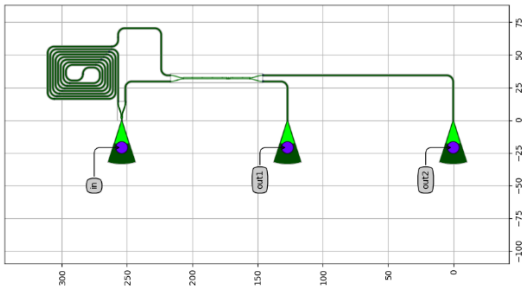

Fig. 6. MZI circuit with 1000um long arm in IPKISS for layout and simulation

```
mzi_1000 = MZI_Spiral(spiral_length=1000, spiral_turns=4, growth_dir="V")
mzi_1000_layout = mzi_1000.Layout()
mzi_1000_layout.visualize(annotate=True)
cm = mzi_1000.CircuitModel()
wavelengths = np.linspace( start: 1.52,  stop: 1.58,  num: 4001)
S_total = cm.get_smatrix(wavelengths=wavelengths)

S_total.visualize(
    term_pairs=[
        ("in:0", "out1:0"),
        ("in:0", "out2:0")
    ],
    scale='dB',
    ylabel="Transmission [dB]",
    xlabel="Wavelength [um]",
    title="1000um MZI"
)
```

Fig. 7. IPKISS Code for Simulating an MZI with a 1000um long arm

The IPKISS code calls the MZI_Spiral PCell which takes in the spiral length, number of turns, and the growth direction of the spiral. We then retrieve the circuit model of the spiral, which is included with the SiEPIC PDK for IPKISS. Then we define the wavelengths we want to simulate over and the number of points in the simulation. We are simulating between 1520nm to 1580nm, and we are sampling 4001 points. The visualize command is used to plot the result of the simulation result. The table below describes the variations we made for our simulations.

Table 1. Waveguide Arm Lengths & ΔL

Top Arm	Bottom Arm	ΔL
10µm	1010µm	1000µm
10 µm	2010µm	2000µm
10 µm	3010µm	3000µm
10 µm	4010µm	4000µm

Figures 8-11 show the simulation results obtained from IPKISS. With the blue line representing the output from port ‘out1’ in the layout. This is goes directly from the splitter and out from the grating coupler. It does not go through the spiral. The orange line represents the output from port ‘out2’. This is the connection that goes through the spiral.

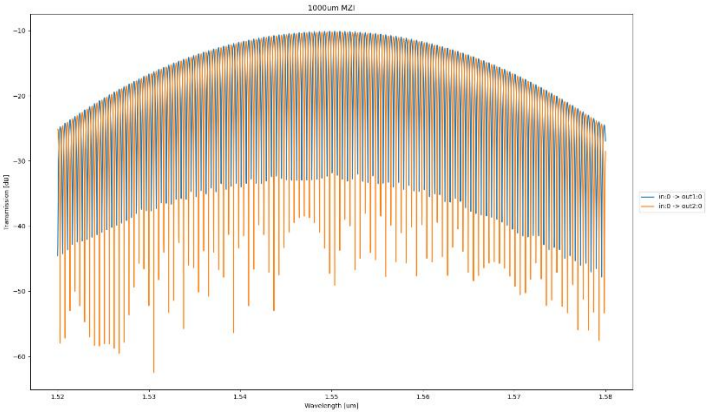

Fig. 8. Simulation results for $\Delta L = 1000$

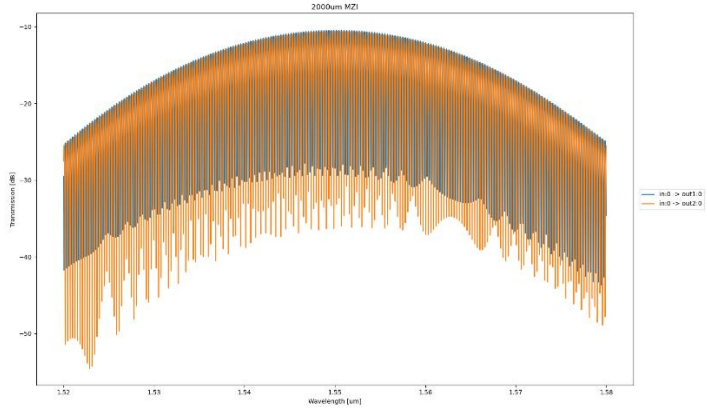

Fig. 9. Simulation results for $\Delta L = 2000$

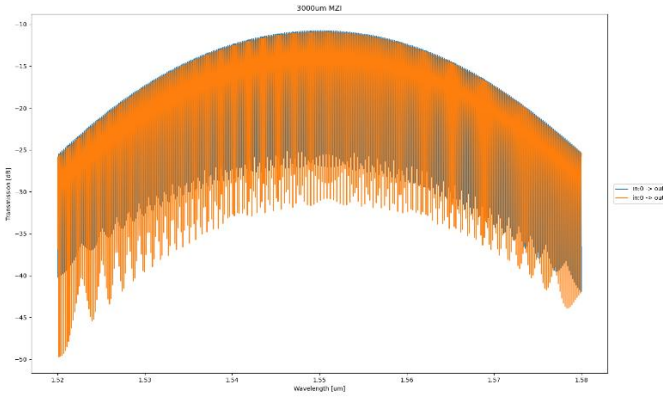

Fig. 10. Simulation results for $\Delta L = 3000$

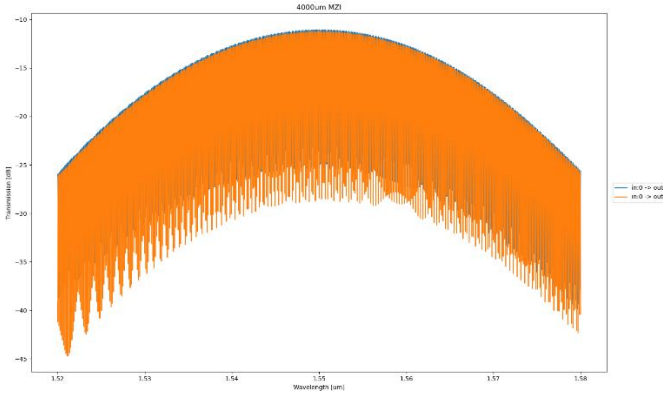

Fig. 11. Simulation results for $\Delta L = 4000$

All the components used in this simulation come from the SiEPIC PDK that comes with IPKISS.

The plots show that the number of oscillations increases as the ΔL grows larger. Which is expected when we observe the equation that gives us the FSR. As the denominator grows, the FSR gets smaller, which can mean more oscillations within a given wavelength range.

Due to spatial constraints on the chip, we will only be able to test four devices and only be able to change one parameter. The table below contains the parameters that we plan to change for this study.

Table 2. Parameters we plan to change for this study

Waveguide Width (nm)	ΔL (µm)	Splitter Type
500	1000, 2000, 3000, 4000	Y-Splitter

This proposed design of experiments will give us a variety of data that will help us to observe how the interferometer behaves when we use very long lengths for the unbalanced arms. We will also be able to extract material data from these MZIs.

IV. Layout, Fabrication & Manufacturing Variability

The layout was made using Luceda IPKISS with the SiEPIC PDK. The layout was then verified using the functional verification and design rule check utility in SiEPIC for KLayout. Figure 12 below shows the layout that was fabricated.

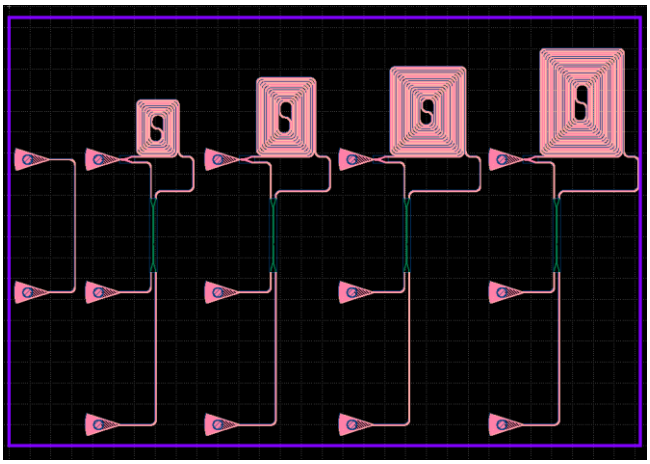

Fig 12. Layout fabricated shown in KLayout

The devices from left to right with their ΔL is shown in the table below.

Table 3. Devices Fabricated

Device	ΔL (µm)
Calibration	N/A
MZI	1000
MZI	2000
MZI	3000
MZI	4000

The devices were fabricated using 100 keV Electron Beam Lithography [1]. The fabrication used silicon-on-insulator wafer with 220 nm thick silicon on 3 µm thick silicon dioxide. The substrates were 25 mm squares diced from 150 mm wafers. After a solvent rinse and hot-plate dehydration bake, hydrogen silsesquioxane resist (HSQ, Dow-Corning XP-1541-006) was spin-coated at 4000 rpm, then hotplate baked at 80 °C for 4 minutes. Electron beam lithography was performed using a JEOL JBX-6300FS system operated at 100 keV energy, 8 nA beam current, and 500 µm exposure field size. The machine grid used for shape placement was 1 nm, while the beam stepping grid, the spacing between dwell points during the shape writing, was 6 nm. An exposure dose of 2800 µC/cm2 was used. The resist was developed by immersion in 25% tetramethylammonium hydroxide for 4 minutes, followed by a flowing deionized water rinse for 60 s, an isopropanol rinse for 10 s, and then blown dry with nitrogen. The silicon was removed from unexposed areas using inductively coupled plasma etching in an Oxford Plasmalab System 100, with a chlorine gas flow of 20 sccm, pressure of 12 mT, ICP power of 800 W, bias power of 40 W, and a platen temperature of 20 °C, resulting in a bias voltage of 185 V. During etching, chips were mounted on a 100 mm silicon carrier wafer using perfluoropolyether vacuum oil. Cladding oxide was deposited

using plasma enhanced chemical vapor deposition (PECVD) in an Oxford Plasmalab System 100 with a silane (SiH4) flow of 13.0 sccm, nitrous oxide (N2O) flow of 1000.0 sccm, high-purity nitrogen (N2) flow of 500.0 sccm, pressure at 1400mT, high-frequency RF power of 120W, and a platen temperature of 350C. During deposition, chips rest directly on a silicon carrier wafer and are buffered by silicon pieces on all sides to aid uniformity.

A fabrication process typically has some sort of variability in the fabrication result, which affects the performance of the devices we are making. The variation in the fabrication process is typically structural variation, rooting from things such as changes in the resist properties, exposure times, lithography, or the temperature and humidity of the cleanroom during fabrication. The Washington University Nanofabrication Facility reports a variation of 470 - 510nm in waveguide width from the nominal value of 500nm, and the silicon thickness of the wafer varies between 215.3 - 223.1nm from the nominal value of 220nm.

We have conducted a corner analysis of our devices to understand the variation in the group index we can expect. The corner analysis was done in Ansys Lumerical MODE with the center wavelength at 1550nm. The table below shows the corners we simulated as well as group index and effective index we found for the fundamental TE mode.

Table 4. Corner Analysis Results for fundamental TE Mode

Corner Variation	Waveguide Width (nm)	Waveguide Height (nm)	Group Index	Effective Index
Nominal	500	220	4.2040	2.4448
1	470	215.3	4.2495	2.3734
2	470	223.1	4.2598	2.4060
3	510	215.3	4.1786	2.4412
4	510	223.1	4.1869	2.4738

The range we can expect in the group index is from 4.1786 - 4.2598, and the range we can expect in effective index is 2.3734 - 2.4738.

The data obtained from the corner analysis can be used to analytically predict the range in FSR using the expression for that we derived earlier in this work. The expected FSR variation at 1550nm can be found in the table below.

Table 5. FSR Variation from Corner Analysis Data

Data Source	ΔL (µm)	FSR (nm)
Corner Analysis	1000	0.564 – 0.575
Nominal	1000	0.5715
Corner Analysis	2000	0.282 – 0.2875
Nominal	2000	0.2857
Corner Analysis	3000	0.188 – 0.1917
Nominal	3000	0.1905
Corner Analysis	4000	0.141 – 0.1437
Nominal	4000	0.1429

V. Measurement & Data Analysis

To characterize the devices, a custom-built automated test setup [2, 6] with automated control software written in Python was used [3]. An Agilent 81600B tunable laser was used as the input source and Agilent 81635A optical power sensors as the output detectors. The wavelength was swept from 1500 to 1600 nm in 10 pm steps. A polarization maintaining (PM) fiber was used to maintain the polarization state of the light, to couple the TE polarization into the grating couplers [4]. A 90º rotation was used to inject light into the TM grating couplers [4]. A polarization maintaining fiber array was used to couple light in/out of the chip [5].

We will first analyze the data of our calibration structure, which is the loop back. This structure, shown below in figure 13, comprises of two grating couplers connected to each other by a waveguide.

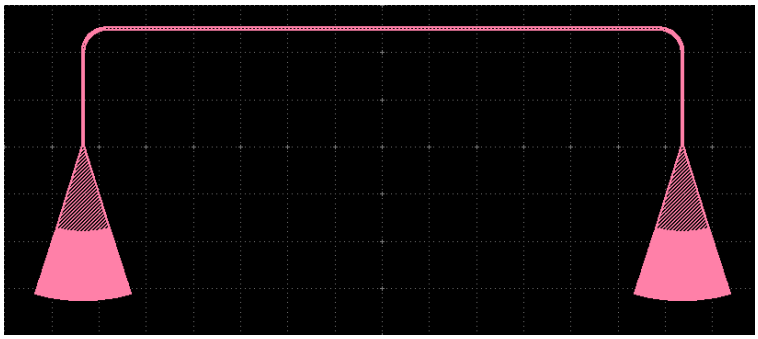

Fig 13. Loopback structure as shown in KLayout

We will be using this loopback structure to eliminate the effects of the grating coupler from our MZI transmission data. To avoid using noisy parts of our data, we will be using a wavelength range with 10dB of loss variation. We then subtract the loss from the transmission spectrum of the MZIs. Figure 14 demonstrates what the transmission spectrum looks like with the wavelength range highlighted for a 10dB loss variation.

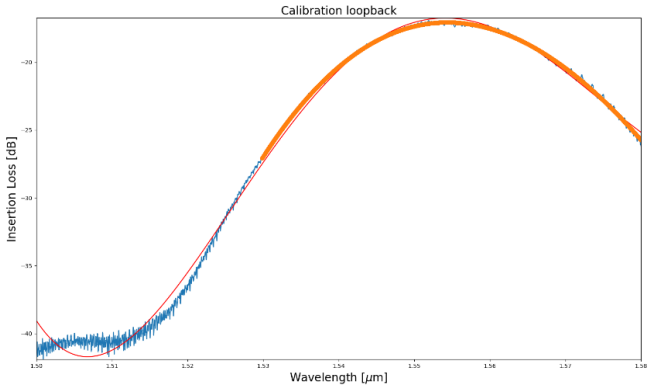

Fig 14. Grating coupler insertion loss calibration
The blue line represents the response of the grating coupler over a wavelength range and the orange line represents the wavelength range with 10dB insertion loss.

After we analyze the loopback structure, we will then analyze the MZI structure. For this work, we will only analyze the MZI where the ΔL = 1000µm. Figure 15 shows this data after calibration and fitting.

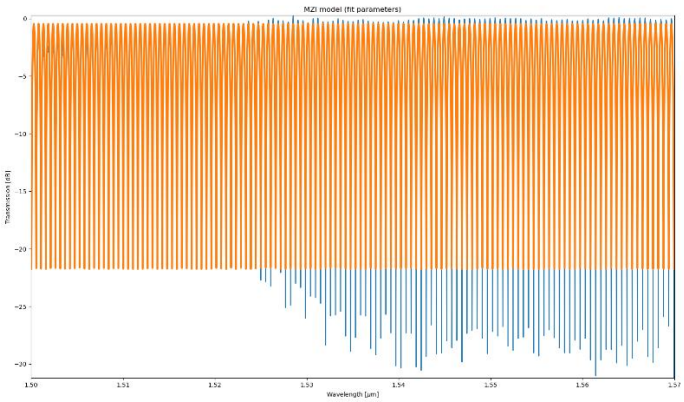

Fig 15. Fitted and calibrated 1000µm MZI transmission spectrum

The blue line here shows the experimental data, and the orange line here shows the fitted data. The table below shows a comparison of the group indices from the corner analysis of a 220 x 550nm waveguide with the group index of the 1000µm MZI. All of this is at 1550nm wavelength.

Table 6. Group Index of 1000µm MZI vs Corner Analysis

Data	Group Index
Corner Analysis Range	4.1786 – 4.2598
1000µm MZI	3.8662

The extracted group index of 3.8595 from the 1000µm MZI is lower than the expected range from the corner analysis. The extracted FSR from this device is 0.5549nm, which is also lower than expected.

VI. Discussion & Summary

There are potentially many reasons why the extracted data falls out of the expected range, though my main suspicion is the bends in the spiral. The 1000µm long delay arm of the MZI comes from a square spiral, which has 4 bends for each rotation in the spiral. A large number of bends can cause the mode to shift, which may be causing our group index to drop. The bend radius we used in our layout is 5µm. While this is fairly normal for balancing compactness and loss in Silicon Photonics, I wonder if a larger bend radius would have gotten us a group index closer to the simulated range.

The waveguide simulations and corner analyses done in Lumerical do not consider the bends in the spiral. This can be improved in the future by making sure to simulate bend effects on the waveguide in Lumerical and inside of a circuit simulator. Luceda IPKISS was used to conduct circuit simulations, while it is a powerful tool, it may not be equipped to simulate bend effects on a waveguide.

The FSR could be out of range due to inaccurate distance between the spiral output and the directional coupler's input heading to the grating coupler. This can be improved in the future by using more accurate methods for measurement of the waveguides.

While we were able to get data that visually is not completely incorrect, the accuracy of the data after processing is still something to investigate. This is mainly due to having to modify the Python based data processing scripts beyond what was suggested to properly read the device data. Both of which were provided by the testing facility. To avoid this in the future, it would make sense to write the scripts myself to ensure that the data is being processed correctly. It could be beneficial to request the correct scripts from the testing facility as well.

The corner analysis was done again at a center wavelength of 1550nm to understand what range of width & height would give us a result that encompasses the extracted group index. The range we have found for the height is 153-223.1nm, and the range for the width is 470-650nm. Table 7 shows the corner vs group index.

Table 7. Group Index for modified Corner Analysis

Corner	Simulated Waveguide Width (nm)	Simulated Waveguide Height (nm)	Group Index
1	470	153	4.0274
2	470	223.1	4.2598
3	650	153	3.8593
4	650	223.1	4.0130
1000µm MZI	**-**	**-**	**3.8662**

We can see that the group index of our measured MZI falls within the range extracted from this corner analysis. I am doubtful that the foundry process has varied by so much from their nominal value, so I suspect that the data analysis scripts or the bends in the spiral are the cause of a lower than expected group index.

In summary, we designed and fabricated a set of devices that have an extreme variation in delay line lengths, made possible by square spirals. Measured the devices and processed the data to extract the device's FSR and group index. We have found a mismatch between the simulated values and the measured values, the cause of which is suspected to be from bends inside of the spiral which may cause the mode to shift, leading to a lower group index. Redoing the corner analysis gives us increased corner values that include the group index we have gotten from the 1000µm MZI. Suggestions such as better data analysis scripts and simulating spirals have been made to further improve upon this work. With the right resources and time, one can certainly produce results that are within range of the simulated values.

ACKNOWLEDGEMENTS

I acknowledge the edX UBCx Phot1x Silicon Photonics Design, Fabrication and Data Analysis course, which is supported by the Natural Sciences and Engineering Research Council of Canada (NSERC) Silicon Electronic-Photonic Integrated Circuits (SiEPIC) Program. The devices were fabricated by Richard Bojko at the University of Washington Washington Nanofabrication Facility, part of the National Science Foundation's National Nanotechnology Infrastructure Network (NNIN), and Cameron Horvath at Applied Nanotools, Inc. Omid Esmaeeli performed the measurements at The University of British Columbia. I acknowledge Lumerical Solutions, Inc., Mathworks, Luceda Photonics, Python, and KLayout for the design software. I acknowledge Spark Photonics Design for funding my seat as a student in this course.

REFERENCES

[1] R. J. Bojko, J. Li, L. He, T. Baehr-Jones, M. Hochberg, and Y. Aida, "Electron beam lithography writing strategies for low loss, high confinement silicon optical waveguides," J. Vacuum Sci. Technol. B 29, 06F309 (2011)

[2] Lukas Chrostowski, Michael Hochberg, chapter 12 in "Silicon Photonics Design: From Devices to Systems", Cambridge University Press, 2015

[3] http://siepic.ubc.ca/probestation, using Python code developed by Michael Caverley.

[4] Yun Wang, Xu Wang, Jonas Flueckiger, Han Yun, Wei Shi, Richard Bojko, Nicolas A. F. Jaeger, Lukas Chrostowski, "Focusing sub-wavelength grating couplers with low back reflections for rapid prototyping of silicon photonic circuits", Optics Express Vol. 22, Issue 17, pp. 20652-20662 (2014) doi: 10.1364/OE.22.020652

[5] www.plcconnections.com, PLC Connections, Columbus OH, USA.

[6] http://mapleleafphotonics.com, Maple Leaf Photonics, Seattle WA, USA.

[7] http://lucedaphotonics.com, Luceda Photonics, Dendermonde, Belgium